

DESCRIPTION OF MULTIPARTICLE PRODUCTION BY GLUON DOMINANCE MODEL ¹

L.N.Abesalashvili, L.T.Akhobadze

Institute High Energy Physics and Informatization, Tbilisi State University, Georgia.

E-mail: abesal@hepi.edu.ge

November 28, 2007

ABSTRACT

The obtained π^- and charged multiplicity distribution parameters of Gluon Dominance Model explain the experimental data in nucleus-nucleus, p nucleus, pd, pp, p antip and $\pi^-(p,n)$ interactions. We have undertaken an attempt to give description in different processes of multiparticle production by means of a unified approach based on quark-gluon picture using the phenomenological hadronization. We have obtained agreement of GDM with experimental data in a very wide energy range.

PACS numbers: 13.75.Cs; 13.85.-t; 21.30.-x; 24.85.+t; 25.70.-z.

Keywords: multiplicity distribution, quark-gluon picture, hadronization.

¹ Talk given at IV International Conference of Physics at the Future Colliders, IHEPI TSU, October 22-26, Tbilisi, Georgia.

Multiparticle production (MP) is one of the important branches in high energy physics [1]. Modern accelerators had made it possible the intensive and detailed study of multiparticle processes. Multiplicity is the number of secondaries n in process MP:

$$A + B \rightarrow a_1 + a_2 + \cdots + a_n \quad (1)$$

Multiplicity distribution (MD) P_n is the ratio cross-section σ_n to $\sigma = \sum_n \sigma_n$ $P_n = \sigma_n / \sigma$.

To describe the MD we have used the probability of producing of n charge particles in Gluon Dominance Model (GDM). GDM studies multiparticle production in lepton and hadron processes. It is based on the QCD and phenomenological scheme of hadronization. The model describes well multiplicity distributions and their moments. It has revealed an active role of gluons in multiparticle production, it also has confirmed the fragmentation mechanism of hadronization in e^+e^- annihilation and its change to recombination mechanism in hadron and nucleus interactions. The GDM explains the shoulder structure of multiplicity distributions. The agreement with Au+Au peripheral collisions data for hadron-pion ratio has been also obtained with this model. Development of GDM allows one to study the multiplicity behavior of p+antip annihilation at tens of GeV.

Heavy ion collisions (HIC) at high energies study strong evidences of quark-gluon plasma (QGP) production [2]. The behavior of bulk variables at lower energies and also a detailed study of hadron interactions supply with understanding of the production mechanism of this new state. At present this analysis is realized at SPS (CERN) [3]. The basic problem of HIC is to describe the systems, consisting of partons or hadrons. Experiments at RHIC have confirmed this collective behavior [4]. In the case of the hadron interaction the new formed medium, named quark-gluon plasma (QGP), won't have such a plenty of constituents. We consider that the evaporation of single partons from separate hot pots (cluster sources) in the system of coliding hadrons, leads to the secondary particles production. This conception was taken as the basis of the Gluon Dominance Model [5÷10]. It is supposed that after the inelastic collisions the part of the energy of the initial impact particles is transformed to the inside energy. Several quarks and gluons become free and form quark-gluon system (QGS). Partons which can produce hadrons are named the active ones. Two schemes were proposed [6,7]. In the first scheme the parton fission inside the QGS is taken into account (the scheme with a branch). If we are not interested in what is going inside QGS, we come to the scheme without

a branch. Reserve quarks remained inside of the leading particles. All of the newly born hadrons were formed by active gluons.

The Poisson distribution was chosen as the simplest multiplicity distribution for active gluons which appeared for the first time after the collision. The number of these gluons fulfils the role of the impact parameter for nucleus. On the second stage some of active gluons can leave QGS ("evaporate") and transform to real hadrons. For the hadronization a sub narrow binomial distribution (BD) was added as follows:

$$P_n = \sum_{m=0}^M C_{mN}^{n-2} (\exp(-\bar{m}) \bar{m}^m / m!) (\bar{n}^h / N)^{n-2} (1 - \bar{n}^h / N)^{mN-(n-2)}, \quad (n > 2), \quad (2)$$

($P_2 = \exp(-\bar{m})$), where C_{mN}^{n-2} - binomial coefficient, m and \bar{m} are the number of secondary gluons and their mean multiplicities. In sum (2) we constrain the maximal possible number of the evaporated gluons equal to $M = 6$. \bar{n}^h and N have the meaning of average multiplicity and a maximum possible number of secondary hadrons formed from the gluon at the stage of hadronization.

The comparison (2) with experimental data [8, 11÷25] (see Fig.1÷9 and tables 6÷12), gives the following parameter values (see Tables 1÷5). The expression (2) describes well the experimental data [8, 11÷25] from 4 GeV/c to 900 GeV (e.g. Fig. 1÷9). The mean gluon multiplicity \bar{m} has a tendency to rise, but slower than the logarithmic one. It is surprising that gluon parameters of hadronization (N, \bar{n}^h) remain constant without considerable deviations in spite of the indirect finding: $N \sim 3 \div 4$ and $\bar{n}^h \sim 1$. Therefore we can draw a conclusion about the universality of gluon hadronization in nucleus-nucleus collisions in the rather wide energy region.

As is shown by the analysis (2) gives better description of $\pi^-(p,n)$, $p(p, \text{antip}, d, \text{nucleus})$ and light nuclei collisions than for heavy nuclei.

In [26] MP is described by means of clan mechanism and emphasizes the gluon nature of clan. GDM allows to give a concrete content for clan. The clan model uses the logarithmic distribution (LD) in a single clan.

At the SPS energy the shoulder structure appears in MD [13]. As it was mentioned in the branch scheme, the gluon fission is strengthened at higher energies. The independent evaporation of gluon sources of hadrons may be realized as single gluons as groups from two and more fission gluons. Following [26] such groups is named clans.

The specific feature of GDM is the dominance of active gluons in MP. We expect the emergence of many of them in nucleus collisions at RHIC and the formation of a new kind of matter (QGP) at high energy. The QGS can be a candidate for this. According to GDM, the active gluons are a basic source of secondary hadrons.

In conclusion one can show GDM may explain experimental data [8, 11÷25] (see Fig. 1÷9 and tables 6÷12) and gives the following parameter values (see Tables 1÷5).

GDM describe well MD pp interactions at the region of (50÷800 GeV/c, 62 GeV) (see Table 3 and fig.5), (π^- , p) interactions at the region of (40÷360 GeV/c (see Table 2 and fig 4). The maximum possible number of secondary hadrons formed from the active gluons N , their mean multiplicity \bar{n}^h increase slowly. A growth of \bar{n}^h in pp interactions indicates a possible change mechanism of hadronization of gluons in comparison with (p antip) annihilation (see Table 4 and figure 6).

The parameter of hadronization $(\bar{n}_{ch})^h$ has a tendency to increase weakly. We consider that parameter $(\bar{n}_{ch})^h$ goes to the limiting value (like saturation). For hadron and nucleus processes a lot of quark pairs from gluons appear almost simultaneously and recombine to various hadrons [27]. The value \bar{n}^h becomes bigger $\sim(2\div3)$, that indicates to the transition from the fragmentation mechanism to the recombination one.

In our research we see that:

1. At the same energy the mean multiplicity of the active gluons \bar{m} , the maximal possible number of secondary hadrons formed from one active gluons at the second stage N and their mean multiplicity \bar{n}^h is higher in the nucleus-nucleus collisions and annihilation processes, than in the hadron-hadron interactions.

2. With the growth of the energy of colliding particles the mean multiplicity of the active gluons \bar{m} increase slowly in all interactions.

We have obtained agreement of Gluon Dominance Model (GDM) with experimental data in (p antip) annihilation, pp, (π^- , (p,n)), pd and nucleus-nucleus collisions in a very wide energy domain.

The specific feature of GDM is the dominance of active gluons in MP. We expect the emergence of many of them in nucleus collisions and the formation of a new kind of matter (QGP) at high energy.

The authors appreciate for the support of physicists from HEPI TSU who encouraged our investigation.

References

- [1] J.Manjavidze and A.N.Sissakyan, Phys. Rep. **346**, 1 (2001).
- [2] C.A. Salgado, Plenary talk at the Conference Physics at LHC, Crakow (Poland), July 2006, hep-ph/0609177.
- [3] C.Blume, to be published in Nucl.Phys. A, nucl-ex/060922.
- [4] I.Arsene et. al., BRAMS collaboration, nucl-ex/0610021.
- [5] V.I.Kuvshinov and E.S.Kokoulina, Acta Phys. Polon. **B13**, 553 (1982).
- [6] E.S.Kokoulina, Acta Phys. Polon. **B35**, 295 (2004);
e-Print Arxive: hep-ph/040123 v1 28 Jan 2004.
- [7] E.S.Kokoulina and V.A.Nikitin, 17th ISHEPP. Dubna, JINR, (2005);
e-Print Arxive: hep-ph/0502224, Feb. 2005.
- [8] E.S.Kokoulina, e-Print Arxive: hep-ph/0511111 Nov. 2005;
e-Print Arxive: hep-ph/0511114 Nov. 2005.
- [9] P.F.Ermolov et. al., 17th ISHEPP. Dubna, JINR, (2005);
e-Print Arxive: hep-ph/0503254 Nov. 2005.
- [10] E.Kokoulina, A.Kutov, V.Nikitin, hep-ph/0612364, Dec. 2006.
- [11] M.Derrick et.al., HRS Collab. ANL-HEP-CP-86-26; Phys.Lett. **B168**, 299 (1986).
- [12] P.Abreu et. al., (DELPHI Collab), Phys. Lett. **B247**, 137 (1990);
Z. Phys. **C50**, 185 (1991); Z. Phys. **C52**, 271 (1991).
- [13] G.J.Alner et. al., Phys. Lett. **B167**, 476 (1986); Phys. Rep. **154**, 247 (1987).
R.E.Ansorge et. al., (UA5 Collab), Z. Phys. **C43**, 357 (1989).
- [14] V.V.Ammosov et. al., Phys. Lett. **42B**, 519 (1972);
V.V.Babintsev et.al., Preprint No. M-25, IHEP (Protvino, 1976).
- [15] O.Bolea et. al., Report "P" 1411/VI/PH, 1972.
A.U.Abdurakhimov et. al., Preprint No. P1-6277, JINR (Dubna, 1972).

- [16] L.N.Abesalashvili et al., Preprint No. E1-7876, JINR (Dubna, 1974);
Published in Phys.Lett. **B52**, 236 (1974).
- [17] L.N.Abesalashvili et al., Bulletin of the Georgian Academy of Sciences
75, No.3, 577 (1974).
- [18] N.Angelov et.al., Preprint No. P1-12281, JINR (Dubna, 1979); Yad.
Fiz. **30**, 1590 (1979).
- [19] C.Bromberg et al., D74-01047, 1973; Phys.Rev.Lett.**31**, 1563 (1973).
- [20] G.N.Agakishiev et al., Preprint No. 1-83-22, JINR (Dubna, 1983).
- [21] G.N.Agakishiev et al., Preprint No. P1-84-35, JINR (Dubna,1984);
Yad. Fiz. **40**, 1209 (1984).
- [22] A.Firestone et. al.,Phys.Rev **D14**, 2902 (1976).
A.Sheng, A.Firestone et.al., Phys.Rev. **D12**, 1219 (1975).
- [23] V.S.Murzin and L.I.Sarycheva, Investigations of high energy hadrons
(Nauka, Moscow, 1983), p.181 and 188.
- [24] C.De Marzo et. al.,Phys. Rev. **D26**, No. 5, 1019 (1982).
- [25] J.G. Rushbrooke and B.R. Webber, Phys. Rep. **C44**, 1 (1978);
E. Klempt et. al., Phys. Rep. **413**, 197 (2005).
- [26] A. Giovannini, Nucl. Phys. **B161**, 429 (1979);
A. Giovannini and R.Ugocioni, hep-ph/0405251, 2004.
- [27] R.C. Hwa and C.B. Yang, Phys. Rev., **C67**, 034902 (2003),
[nucl-th/0211010];
R.C. Hwa, ISMD2004 [nucl-th/0410003]; B.Muller, [nucl-th/0404015]
(2004);
U.Heinz, [nucl-th/0407067] (2004);
P.Sorensen, Subm. to J. Phys. G: Nucl. Phys., [nucl-exp/0412003]

FIGURE CAPTIONS

Fig.1. The multiplicity distributions of π^- mesons in $((\text{He},d,C),\text{Ta})$ collisions at 4.2 GeV/ c /nucleon. The curves are the result of the approximation of experimental data by sum (2) of Gluon Dominance Model.

Fig.2. The multiplicity distributions of π^- mesons in $((\text{He},C),C)$ collisions at 4.2 GeV/ c /nucleon. The curves are the result of the approximation of experimental data by sum (2) of Gluon Dominance Model.

Fig.3. The multiplicity distributions of π^- mesons in $((\text{He},C),\text{Prop})$ collisions at 4.2 GeV/ c /nucleon. The curves are the result of the approximation of experimental data by sum (2) of Gluon Dominance Model.

Fig.4. The multiplicity distributions of charged particles in $(\pi^-,p)\rightarrow(\text{ch},X)$ at (40, 50, 205 and 360) GeV/ c . The curves are the result of the approximation of experimental data by sum (2) of Gluon Dominance Model.

Fig.5. The multiplicity distributions of charged particles in $(p,p)\rightarrow(\text{ch},X)$ at (50,300 and 800) GeV/ c . The curves are the result of the approximation of experimental data by sum (2) of Gluon Dominance Model.

Fig.6. The multiplicity distributions of charged particles in $(p,\text{antip})\rightarrow(\text{ch},X)$ at (14.75 and 22.4) GeV/ c . The curves are the result of the approximation of experimental data by sum (2) of Gluon Dominance Model.

Fig.7. The multiplicity distributions of charged particles $(\pi^-,n)\rightarrow(\text{ch},X)$ at the momentum of 40 GeV/ c /nucleon and $(p,(p,n,d))\rightarrow(\text{ch},X)$ at the momentum of 300 GeV/ c /nucleon. The curves are the result of the approximation of experimental data by sum (2) of Gluon Dominance Model.

Fig.8. The multiplicity distributions of π^- mesons in $(p,(\text{Ar},\text{Xe}))\rightarrow(\pi^-,X)$ collisions at 200 GeV/ c /nucleon. The curves are the result of the approximation of experimental data by sum (2) of Gluon Dominance Model.

Fig.9. The multiplicity distributions of charged particles in $(p,(\text{Ar},\text{Xe}))\rightarrow(\text{ch},X)$ collisions at 200 GeV/ c /nucleon. The curves are the result of the approximation of experimental data by sum (2) of Gluon Dominance Model.

Table 1. Parameters of gluon dominance model (GDM)
 $(\text{He}, d, \text{C})\text{Ta} \rightarrow (\pi^-, \text{X}), (\text{C}, \text{Ta}) \rightarrow (\text{ch}, \text{X}), (\text{He}, \text{C})\text{C} \rightarrow (\pi^-, \text{X})$ and
 $(\text{He}, \text{C})\text{Prop} \rightarrow (\pi^-, \text{X})$ at the momentum of 4.2 GeV/c/nucleon.

A_P Projectile and A_T target

A_P, A_T	\bar{m}	N	\bar{n}^h	χ^2/ndf	χ^2/N_{exp}
(He, Ta)	2.34 ± 0.12	10.21 ± 2.54	3.99 ± 0.49	17/5	17/8
(d, Ta)	2.82 ± 0.22	12.50 ± 4.92	4.42 ± 0.69	10/3	10/6
$(\text{C}, \text{Ta}) \rightarrow (\pi^-, \text{X})$	2.81 ± 0.08	5.03 ± 0.27	1.97 ± 0.10	8/6	11/6
$(\text{C}, \text{Ta}) \rightarrow (\text{ch}, \text{X})$	3.84 ± 0.13	5.92 ± 0.38	2.23 ± 0.13	14/12	14/15
(He, C)	2.89 ± 0.21	10.23 ± 3.04	5.40 ± 0.49	11/3	11/6
(C, C)	2.34 ± 0.13	12.40 ± 5.90	5.14 ± 1.49	15/5	15/8
$(He, Prop)$	$1.93.67 \pm 0.31$	10.07 ± 4.28	5.74 ± 1.96	5/3	5/6
$(C, Prop)$	2.86 ± 0.12	12.49 ± 5.26	5.13 ± 2.01	14/5	14/8

Table 2. Parameters of gluon dominance model (GDM) $(\pi^-, p) \rightarrow (\text{ch}, \text{X})$
at the momentum of (40, 50, 205 and 360) GeV/c.

A_P Projectile π^- and A_T target p

A_P, A_T	\bar{m}	N	\bar{n}^h	χ^2/ndf	χ^2/N_{exp}
40 GeV/c	1.41 ± 0.10	2.00 ± 0.01	1.36 ± 0.06	6/6	6/9
50 GeV/c	2.61 ± 0.68	1.00 ± 0.01	0.74 ± 0.20	3/5	3/8
205 GeV/c	4.29 ± 0.12	2.84 ± 0.43	0.81 ± 0.15	10/7	10/10
360 GeV/c	4.34 ± 0.17	4.47 ± 1.22	0.90 ± 0.02	4.4/8	4.4/11

Table 3. Parameters of gluon dominance model (GDM)
 $(p, p) \rightarrow (\text{ch}, \text{X})$ at (50, 200, 205, 300, 400 and 800) GeV/c and at 62 GeV.

A_P Projectile p and A_T target p

A_P, A_T	\bar{m}	N	\bar{n}^h	χ^2/ndf	χ^2/N_{exp}
50 GeV/c	2.35 ± 0.60	2.00 ± 0.17	1.46 ± 0.09	6/4	6/7
200 GeV/c	3.13 ± 0.26	1.91 ± 0.25	0.97 ± 0.06	14/7	14/10
205 GeV/c	2.91 ± 0.21	2.01 ± 0.16	1.01 ± 0.05	16/8	16/11
300 GeV/c	3.35 ± 0.29	5.27 ± 3.03	1.21 ± 0.09	13/9	13/12
400 GeV/c	2.24 ± 0.91	2.28 ± 0.11	1.31 ± 0.06	19/12	19/15
800 GeV/c	2.66 ± 0.16	2.25 ± 0.07	1.29 ± 0.04	16/13	16/16
62 GeV	2.33 ± 0.11	3.23 ± 0.17	1.95 ± 0.08	24/15	24/18

Table 4. Parameters of gluon dominance model (GDM)
 $(p, \text{antip}) \rightarrow (\text{ch}, X)$ at the momentum of (14.75, 22.4) GeV/c and at (200, 900) GeV.

A_P Projectile p and A_T target antip

A_P, A_T	\bar{m}	N	\bar{n}^h	χ^2/ndf	χ^2/N_{exp}
14.7 GeV/c	2.20±0.18	2.05±0.10	1.21±0.04	1/9	1/12
22.4 GeV/c	2.26±0.18	2.01±0.05	1.33±0.05	8/8	8/11
200 GeV	3.59±0.17	3.00±0.20	1.67±0.05	45/16	45/19
900 GeV	5.68±0.01	4.11±0.70	1.27±0.01	13/8	13/11

Table 5. Parameters of gluon dominance model (GDM)
 $(\pi^-, n) \rightarrow (\text{ch}, X)$ at the momentum of 40 GeV/c,
 $(p, (\text{Ar}, \text{Xe})) \rightarrow (\text{ch}, X)$, $(p, (\text{Ar}, \text{Xe})) \rightarrow (\pi^-, X)$ at the momentum of 200 GeV/c
and $(p, (n, d)) \rightarrow (\text{ch}, X)$ at the momentum of 300 GeV/c/nucleon.

A_P Projectile and A_T target

A_P, A_T	\bar{m}	N	\bar{n}^h	χ^2/ndf	χ^2/N_{exp}
$(\pi^-, n) \rightarrow (\text{ch}, X) 40$	1.45±0.12	2.71±0.13	1.67±0.13	6/5	6/8
$(p, n) \rightarrow (\text{ch}, X) 300$	2.44±0.13	2.41±0.11	1.40±0.01	13/9	13/12
$(p, d) \rightarrow (\text{ch}, X) 300$	2.65±0.12	3.33±0.15	2.14±0.01	10/9	10/12
$(p, \text{Ar}) \rightarrow (\text{ch}, X) 200$	3.40±0.10	5.00±0.43	3.27±0.01	43/17	43/20
$(p, \text{Xe}) \rightarrow (\text{ch}, X) 200$	5.64±0.33	4.83±0.02	3.19±0.03	58/11	58/14
$(p, \text{Ar}) \rightarrow (\pi^-, X) 200$	2.25±0.14	2.51±0.14	1.58±0.1	31/19	31/22
$(p, \text{Xe}) \rightarrow (\pi^-, X) 200$	2.32±0.11	3.00±0.02	1.98±0.02	31/19	31/22

Table 6. Experimental results the multiplicity distributions of π^- mesons and of charged particles in ((He,d,C)Ta) collisions at 4.2 GeV/c/nucleon [20]

Mult	(d,Ta)	(He,Ta)	(C,Ta)	(C,Ta) \rightarrow (ch,X)	Mult	(C,Ta)
n	Pn \pm dPn	Pn \pm dPn	Pn \pm dPn	Pn \pm dPn	n	Pn \pm dPn
0	.384 \pm .02	.274 \pm .032	.174 \pm .026	.053 \pm .01	24	.017 \pm .005
1	.376 \pm .02	.341 \pm .022	.194 \pm .015	.094 \pm .01	25	.012 \pm .005
2	.185 \pm .02	.208 \pm .018	.122 \pm .012	.087 \pm .01	26	.010 \pm .004
3	.048 \pm .01	.124 \pm .014	.100 \pm .01	.068 \pm .009	27	.009 \pm .004
4	.004 \pm .002	.043 \pm .012	.083 \pm .01	.054 \pm .008	28	.013 \pm .004
5	.002 \pm .001	.006 \pm .0025	.083 \pm .01	.046 \pm .008	29	.009 \pm .004
6	.001 \pm .001	.003 \pm .0015	.071 \pm .01	.034 \pm .007	30	.011 \pm .004
7	0.	.001 \pm .001	.066 \pm .008	.026 \pm .007	31	.013 \pm .004
8	0.		.049 \pm .008	.029 \pm .007	32	.007 \pm .004
9	0.		.015 \pm .007	.029 \pm .007	33	.007 \pm .004
10			.016 \pm .007	.028 \pm .007	34	.011 \pm .004
11			.011 \pm .005	.019 \pm .007	35	.008 \pm .004
12			.009 \pm .005	.025 \pm .006	36	.010 \pm .004
13			.004 \pm .003	.023 \pm .006	37	.008 \pm .004
14			.009 \pm .008	.023 \pm .006	38	.006 \pm .003
15			.001 \pm .001	.019 \pm .005	39	.009 \pm .004
16				.017 \pm .005	40	.006 \pm .004
17				.023 \pm .005	41	.008 \pm .004
18				.015 \pm .005	42	.003 \pm .002
19				.021 \pm .005	43	.008 \pm .004
20				.012 \pm .005	44	.005 \pm .003
21				.009 \pm .005	45	.004 \pm .002
22				.014 \pm .005	46	.004 \pm .002
23				.010 \pm .005	47	.003 \pm .003

Table 7. Experimental results the multiplicity distributions of π^- mesons in (C,C), ((C,He)Prop) and (He,C) collisions at 4.2 GeV/c/nucleon [21]

Mult	(C,C)	(C,Prop)	(He,Prop)	(He,C)
n	Pn \pm dPn	Pn \pm dPn	Pn \pm dPn	Pn \pm dPn
0	0.177 \pm 0.08	0.417 \pm 0.04	0.482 \pm 0.055	0.349 \pm 0.018
1	0.375 \pm 0.04	0.327 \pm 0.025	0.369 \pm 0.045	0.419 \pm 0.028
2	0.256 \pm 0.03	0.153 \pm 0.015	0.108 \pm 0.035	0.166 \pm 0.017
3	0.097 \pm 0.02	0.053 \pm 0.008	0.030 \pm 0.02	0.048 \pm 0.009
4	0.063 \pm 0.02	0.034 \pm 0.005	0.01 \pm 0.007	0.015 \pm 0.005
5	0.024 \pm 0.006	0.013 \pm 0.003	0.002 \pm 0.0017	0.003 \pm 0.0015
6	0.005 \pm 0.0025	0.0028 \pm 0.0015	0.0	
7	0.003 \pm 0.0015	0.0014 \pm 0.0007	0.0	

Table 8. Experimental results the multiplicity distributions of charged particles

in (π^-, n) collisions at 40 GeV/c [15,17-18], (π^-, p) collisions at 40 GeV/c [15,17-18] and at (50,205 and 360)GeV/c [22]

Mult	$(\pi^-, n)40$	$(\pi^-, p)40$	50 GeV/c	Mult	205 GeV/c	360 GeV/c
n	Pn \pm dPn	Pn \pm dPn	Pn \pm dPn	n	Pn \pm dPn	Pn \pm dPn
0	0.	.050 \pm .030	.007 \pm .001	0	.012 \pm .005	.020 \pm .010
1	.100 \pm .03	0.	0.	2	.069 \pm .005	.059 \pm .009
2	0.	.145 \pm .025	.133 \pm .013	4	.146 \pm .007	.126 \pm .009
3	.271 \pm .03	0.	0.	6	.162 \pm .008	.140 \pm .009
4	0.	.296 \pm .025	.291 \pm .015	8	.171 \pm .008	.156 \pm .009
5	.259 \pm .03	0.	0.	10	.138 \pm .007	.136 \pm .008
6	0.	.263 \pm .025	.270 \pm .013	12	.091 \pm .003	.101 \pm .005
7	.199 \pm .04	0.	0.	14	.046 \pm .004	.065 \pm .004
8	0.	.158 \pm .025	.181 \pm .009	16	.026 \pm .007	.035 \pm .002
9	.107 \pm .04	0.	0.	18	.013 \pm .002	.020 \pm .001
10	0.	.074 \pm .020	.078 \pm .006	20	.004 \pm .002	.010 \pm .001
11	.05 \pm .03	0.	0.	22	.0011 \pm .0004	.004 \pm .001
12	0.	.028 \pm .009	.033 \pm .007	24	.0012 \pm .0004	.002 \pm .001
13	.013 \pm .01	0.	0.	26	.0012 \pm .0004	.001 \pm .0005
14	0.	.008 \pm .004	.006 \pm .002	28	0.	.0002 \pm .0001
15	.003 \pm .001	0.	0.	30	0.	.0001 \pm .0001
16	0.	.002 \pm .001	.003 \pm .0015			
17	.001 \pm .001	0.	0.			
18	0.	.001 \pm .0005	.003 \pm .003			
19	.001 \pm .001	0.	0.			
20	0.	.001 \pm .0003	0.			
22	0.	.0002 \pm .0002	0.			

Table 9. Experimental results the multiplicity distributions of charged particles
in (p,p) collisions at 62 GeV and at (50,200,205,400,800) GeV/ c [14,23-24]

Mult	(p,p) 50	62 GeV	200 GeV/ c	205 GeV/ c	400 GeV/ c	800 GeV/ c
n	Pn \pm dPn	Pn \pm dPn	Pn \pm dPn	Pn \pm dPn	Pn \pm dPn	Pn \pm dPn
2	.158 \pm .014	.047 \pm .015	.075 \pm .015	.107 \pm .015	.082 \pm .020	.045 \pm .015
4	.249 \pm .010	.093 \pm .015	.175 \pm .010	.170 \pm .007	.140 \pm .010	.120 \pm .020
6	.212 \pm .009	.103 \pm .015	.200 \pm .010	.212 \pm .008	.156 \pm .010	.150 \pm .020
8	.133 \pm .006	.113 \pm .015	.200 \pm .010	.177 \pm .007	.174 \pm .010	.160 \pm .020
10	.054 \pm .003	.115 \pm .010	.145 \pm .010	.135 \pm .006	.143 \pm .010	.150 \pm .020
12	.013 \pm .002	.112 \pm .010	.100 \pm .010	.105 \pm .005	.116 \pm .010	.120 \pm .020
14	.005 \pm .001	.108 \pm .010	.005 \pm .005	.052 \pm .003	.085 \pm .010	.100 \pm .020
16	0.	.085 \pm .010	.025 \pm .005	.027 \pm .002	.040 \pm .010	.080 \pm .015
18	0.	.065 \pm .005	.013 \pm .004	.010 \pm .001	.029 \pm .010	.040 \pm .015
20	0.	.053 \pm .005	.005 \pm .002	.005 \pm .001	.017 \pm .009	.025 \pm .008
22	0.	.035 \pm .006	0.	.002 \pm .001	.010 \pm .005	.015 \pm .007
24	0.	.027 \pm .003			.004 \pm .002	.016 \pm .008
26	0.	.020 \pm .003			.0009 \pm .0005	.004 \pm .0015
28	0.	.010 \pm .003			.0005 \pm .0003	.002 \pm .0006
30	0.	.006 \pm .002			.0009 \pm .0005	.0008 \pm .0003
32	0.	.005 \pm .002				.0006 \pm .0003
34	0.	.003 \pm .002				
36	0.	.002 \pm .001				

Table 10. Experimental results the multiplicity distributions of charged particles in (p,antip) collisions at (14.75[8,25], 22.4[16]) GeV/ c and at (200, 900) GeV[13]

Mult	14.75 GeV/ c	22.4 GeV/ c	200 GeV	Mult	900 GeV
n	Pn \pm dPn	Pn \pm dPn	Pn \pm dPn	n	Pn \pm dPn
0	0.050 \pm 0.030	0.017 \pm 0.010	0.	0	0.
2	0.250 \pm 0.080	0.225 \pm 0.055	0.011 \pm 0.008	2	0.010 \pm 0.0015
4	0.080 \pm 0.025	0.362 \pm 0.045	0.045 \pm 0.009	4	0.030 \pm 0.006
6	0.300 \pm 0.090	0.242 \pm 0.024	0.064 \pm 0.006	6	0.060 \pm 0.006
8	0.200 \pm 0.060	0.109 \pm 0.015	0.080 \pm 0.006	8	0.074 \pm 0.007
10	0.050 \pm 0.020	0.036 \pm 0.009	0.100 \pm 0.010	14	0.087 \pm 0.008
12	0.008 \pm 0.002	0.010 \pm 0.004	0.098 \pm 0.009	16	0.090 \pm 0.009
14	0.001 \pm 0.0005	0.002 \pm 0.001	0.102 \pm 0.008	24	0.080 \pm 0.008
16	0.0002 \pm 0.0001	0.0001 \pm 0.0001	0.098 \pm 0.006	34	0.060 \pm 0.006
18	0.	0.	0.094 \pm 0.006	40	0.040 \pm 0.004
20	0.	0.	0.086 \pm 0.006	48	0.030 \pm 0.003
22	0.	0.	0.088 \pm 0.006	50	0.010 \pm 0.002
24	0.		0.076 \pm 0.007		0.
26	0.		0.072 \pm 0.007		
28	0.		0.045 \pm 0.008		
30	0.		0.050 \pm 0.008		
32	0.		0.028 \pm 0.009		
34	0.		0.010 \pm 0.005		
36	0.		0.005 \pm 0.002		0.

Table 11. Experimental results the multiplicity distributions of charged particles in ((p,p),(p,n),(p,d))[22],(p,Ar) and (p,Xe) \rightarrow (π^- ,X)[24]

Mult	(p,p) 300	(p,n) 300	(p,d) 300	(p,Ar) 200	(p,Xe) 200 GeV/c
n	Pn \pm dPn	Pn \pm dPn	Pn \pm dPn	Pn \pm dPn	Pn \pm dPn
0	0.	0.	0.	0.	.025 \pm .015
1	0.	.061 \pm .015	.040 \pm 0.015	0.	0.
2	.063 \pm 0.015	0.	.061 \pm 0.015	.027 \pm .008	.060 \pm .020
3	0.	.121 \pm .012	.110 \pm 0.015	0.	.080 \pm .020
4	.130 \pm 0.010	0.	.130 \pm 0.015	.035 \pm .006	.075 \pm .020
5	0.	.138 \pm .011	0.	0.	.115 \pm .020
6	.139 \pm 0.011	0.	.120 \pm 0.010	0.	.117 \pm .020
7	0.	.147 \pm .015	0.	.041 \pm .006	.110 \pm .020
8	.161 \pm 0.015	0.	0.	0.	.075 \pm .020
9	0.	.130 \pm .013	.094 \pm 0.007	0.	.060 \pm .020
10	.135 \pm 0.014	0.	0.	.057 \pm .006	.052 \pm .020
11	0.	.107 \pm .008	0.	0.	.045 \pm .010
12	.101 \pm 0.013	0.	.073 \pm 0.007	0.	.035 \pm .008
13	0.	.067 \pm .007	0.	.045 \pm .006	.025 \pm .007
14	.062 \pm 0.010	0.	0.	0.	.020 \pm .006
15	0.	.044 \pm .006	.058 \pm 0.007	0.	.015 \pm .006
16	.036 \pm 0.008	0.	0.	.038 \pm .006	.013 \pm .006
17	0.	.018 \pm .005	0.	0.	.012 \pm .006
18	.010 \pm 0.005	0.	.048 \pm 0.007	0.	.011 \pm .006
19	0.	.006 \pm .002	0.	.029 \pm .006	.010 \pm .006
20	.009 \pm 0.004	0.	.029 \pm 0.005	0.	.010 \pm .006
21	0.	.0063 \pm .003	.015 \pm 0.006	0.	.010 \pm .006
22	.003 \pm .0015	0.	.006 \pm 0.003	.028 \pm .006	.012 \pm .007
23	0.	.002 \pm .001	0.	0.	0.
24	.002 \pm 0.001	0.	0.	0.	0.
25	0.	0.	0.	.011 \pm .006	0.
27	0.	0.	0.	0.	0.
28	0.	0.	0.	.016 \pm .006	0.
29	0.	0.	0.	0.	0.
31	0.	0.	0.	.009 \pm .004	0.
34	0.	0.	0.	.008 \pm .004	0.
37	0.	0.	0.	.007 \pm .004	0.
40	0.	0.	0.	.006 \pm .003	0.

Table 12. Experimental results the multiplicity distributions of charged particles in (p,Xe) and (p,Ar) $\rightarrow(\pi^-,X)$ collisions [24]

Mult	(p,Xe)ch 200	Mult	(p,Xe)ch 200	Mult	(p,Ar) $\rightarrow(\pi^-,X)$ 200 GeV/ c
n	Pn \pm dPn	n	Pn \pm dPn	n	Pn \pm dPn
0	0.	31	0.014 \pm 0.006	0	0.025 \pm 0.015
1	0.	34	0.017 \pm 0.006	1	0.
2	0.019 \pm 0.008	37	0.011 \pm 0.005	2	0.080 \pm 0.020
3	0.	40	0.011 \pm 0.005	3	0.100 \pm 0.020
4	0.027 \pm 0.007	43	0.011 \pm 0.005	4	0.130 \pm 0.020
5	0.	46	0.008 \pm 0.004	5	0.150 \pm 0.020
6	0.	49	0.007 \pm 0.004	6	0.120 \pm 0.020
7	0.035 \pm 0.007	52	0.005 \pm 0.003	7	0.100 \pm 0.020
8	0.	55	0.004 \pm 0.003	8	0.070 \pm 0.020
9	0.	58	0.003 \pm 0.002	9	0.050 \pm 0.020
10	0.033 \pm 0.006	60	0.003 \pm 0.002	10	0.035 \pm 0.010
11	0.		0.	11	0.030 \pm 0.010
12	0.		0.	12	0.025 \pm 0.006
13	0.035 \pm 0.006		0.	13	0.013 \pm 0.006
14	0.		0.	14	0.011 \pm 0.006
15	0.		0.	15	0.010 \pm 0.006
16	0.033 \pm 0.006		0.	16	0.011 \pm 0.006
17	0.		0.		
18	0.		0.		
19	0.027 \pm 0.006		0.		
20	0.		0.		
21	0.		0.		
22	0.023 \pm 0.006		0.		
23	0.		0.		
24	0.		0.		
25	0.018 \pm 0.006		0.		
26	0.		0.		
27	0.		0.		
28	0.016 \pm 0.006		0.		
29	0.		0.		
30	0.		0.		

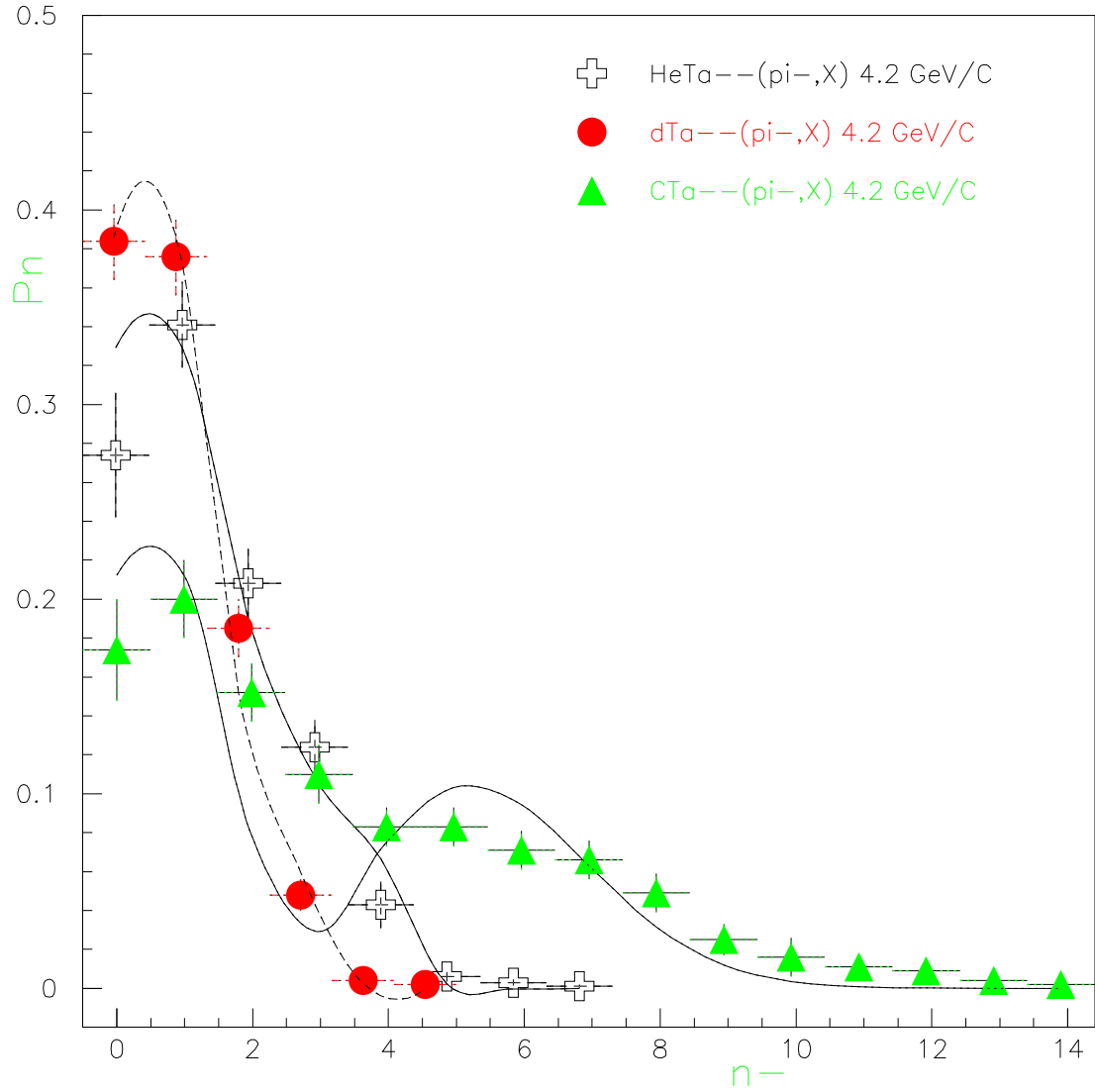


Figure 1: The multiplicity distributions of π^- mesons in $((\text{He}, \text{d}, \text{C}), \text{Ta})$ collisions at 4.2 GeV/c/nucleon.

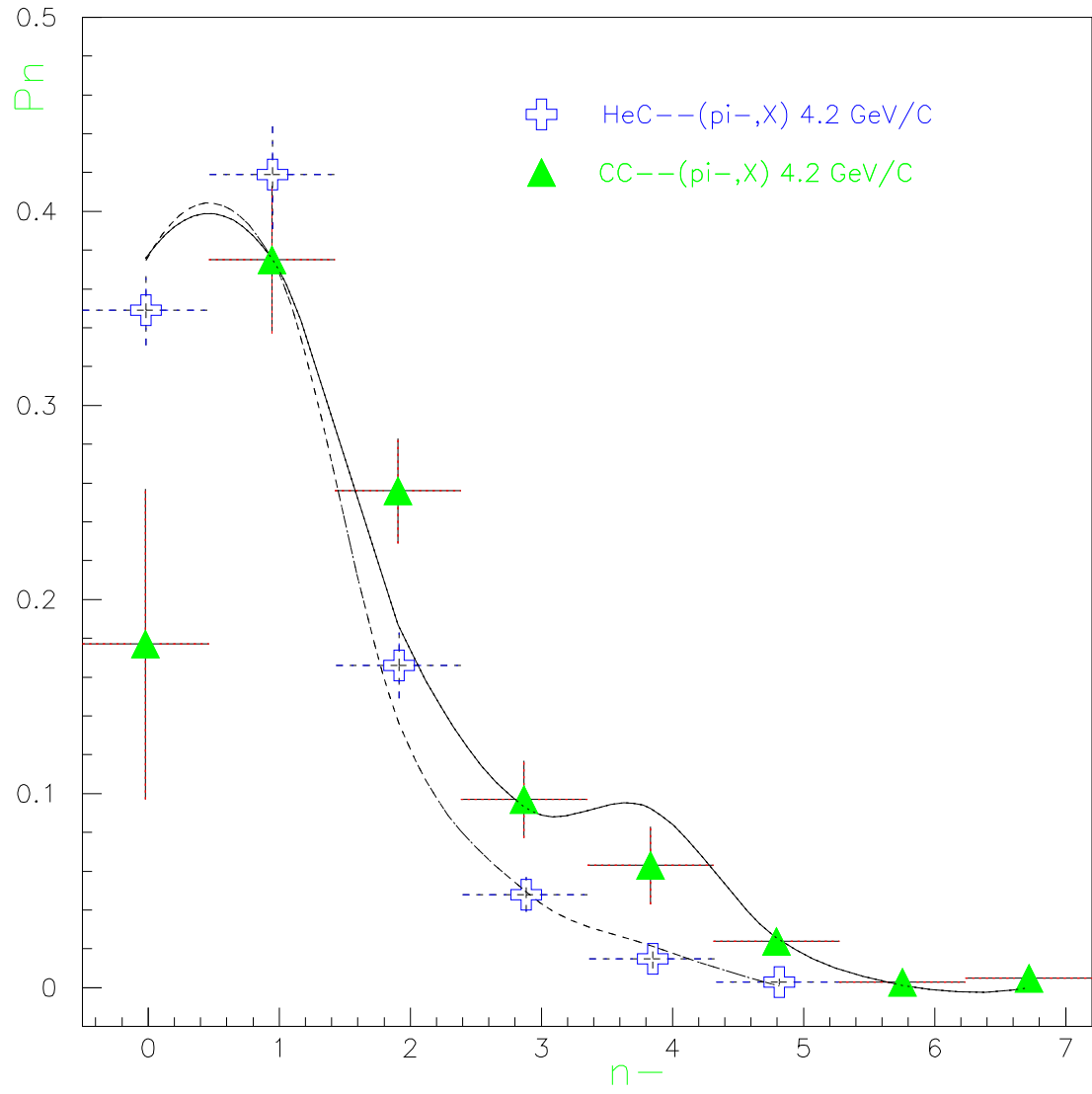


Figure 2: The multiplicity distributions of π^- mesons in $((\text{He}, \text{C}), \text{C})$ collisions at 4.2 GeV/c/nucleon.

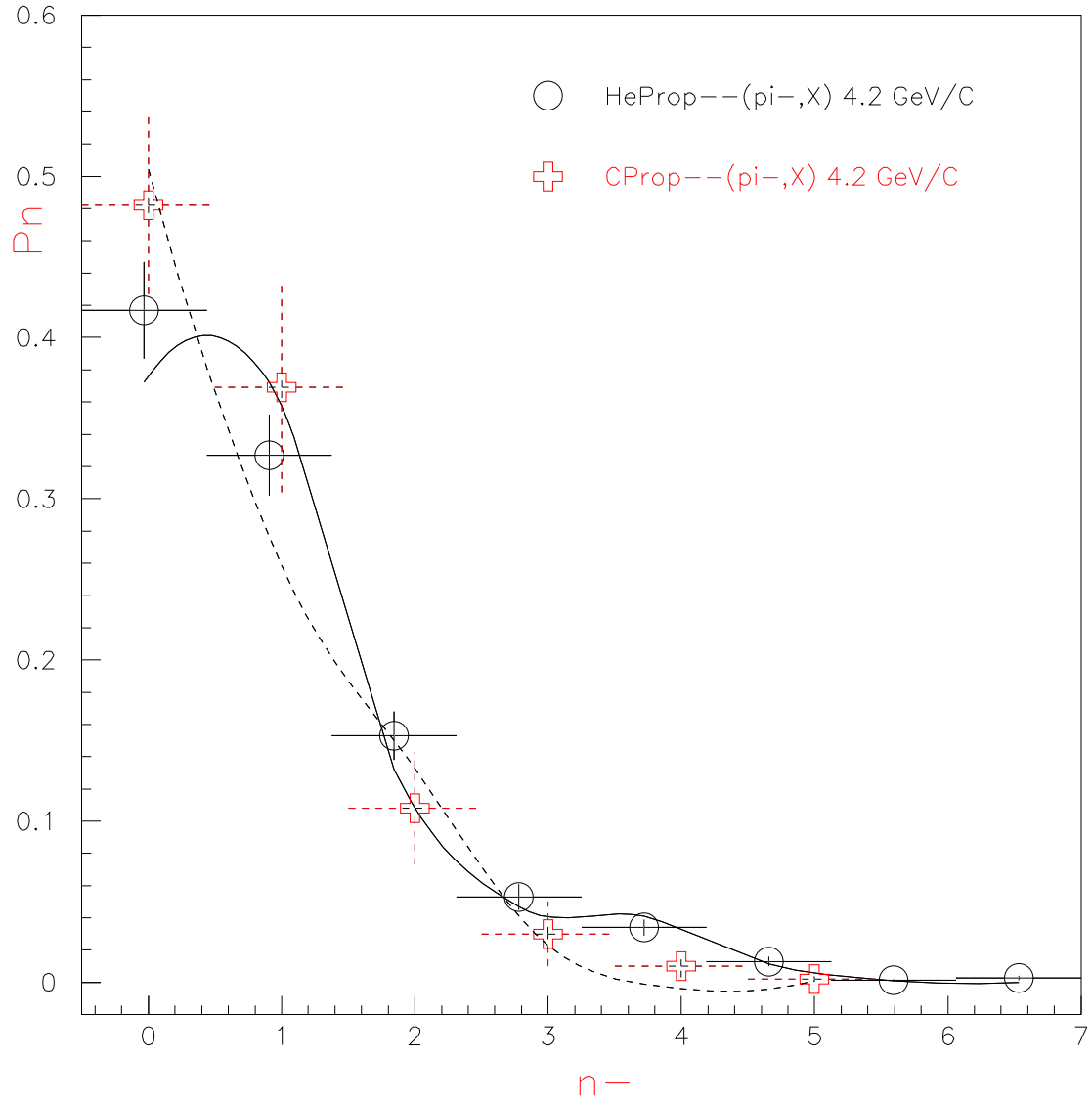


Figure 3: The multiplicity distributions of π^- mesons in $((\text{He}, \text{C}), \text{Prop})$ collisions at 4.2 GeV/c/nucleon.

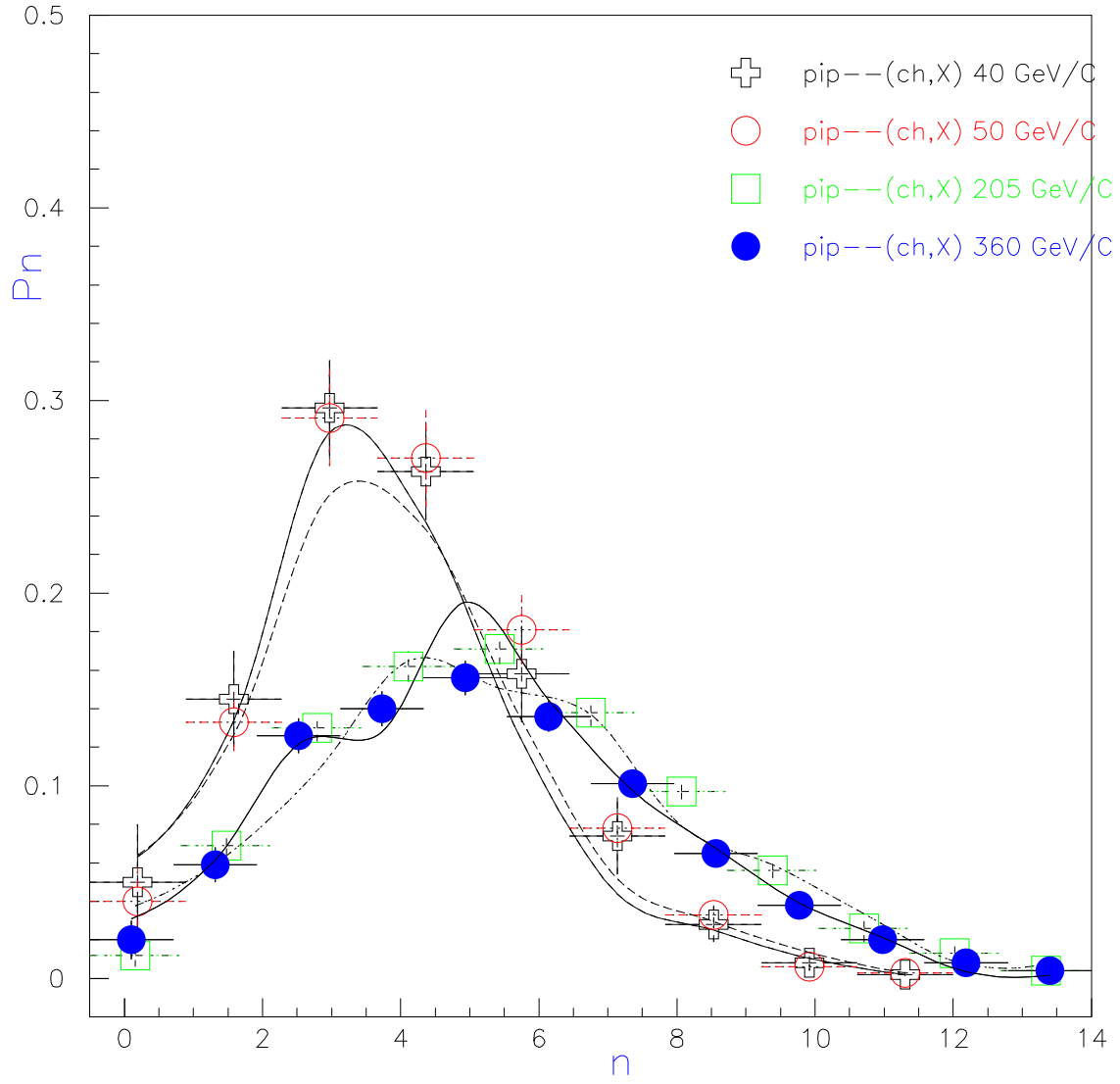


Figure 4: The multiplicity distributions of charged particles in $(\pi^-, p) \rightarrow (ch, X)$ at (40, 50, 205 and 360) GeV/c.

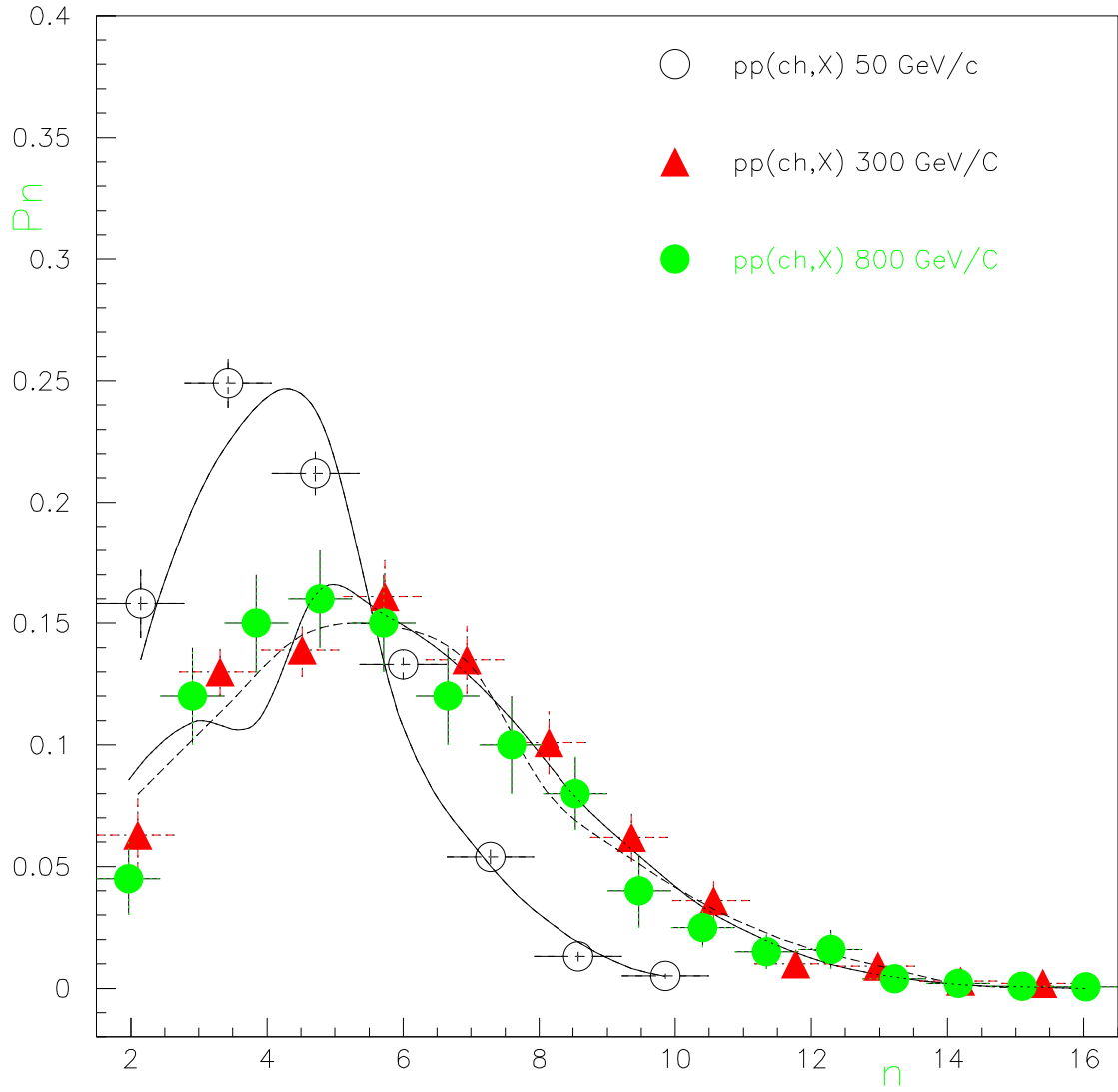


Figure 5: The multiplicity distributions of charged particles in $(p,p) \rightarrow (ch,X)$ at (50,300 and 800) GeV/c.

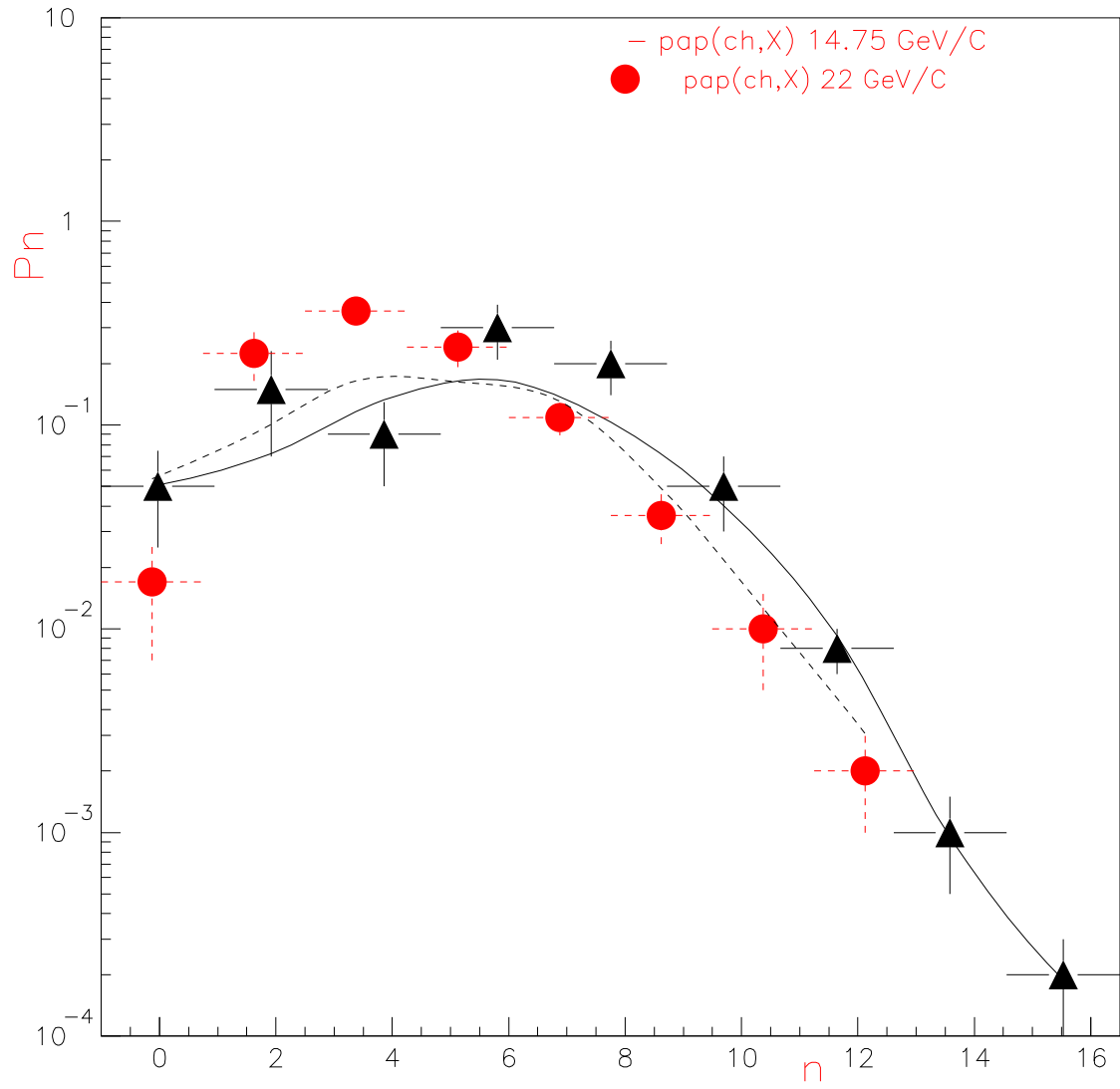


Figure 6: The multiplicity distributions of charged particles in $(p, \text{anti}p) \rightarrow (\text{ch}, X)$ at (14.75 and 22.4) GeV/c.

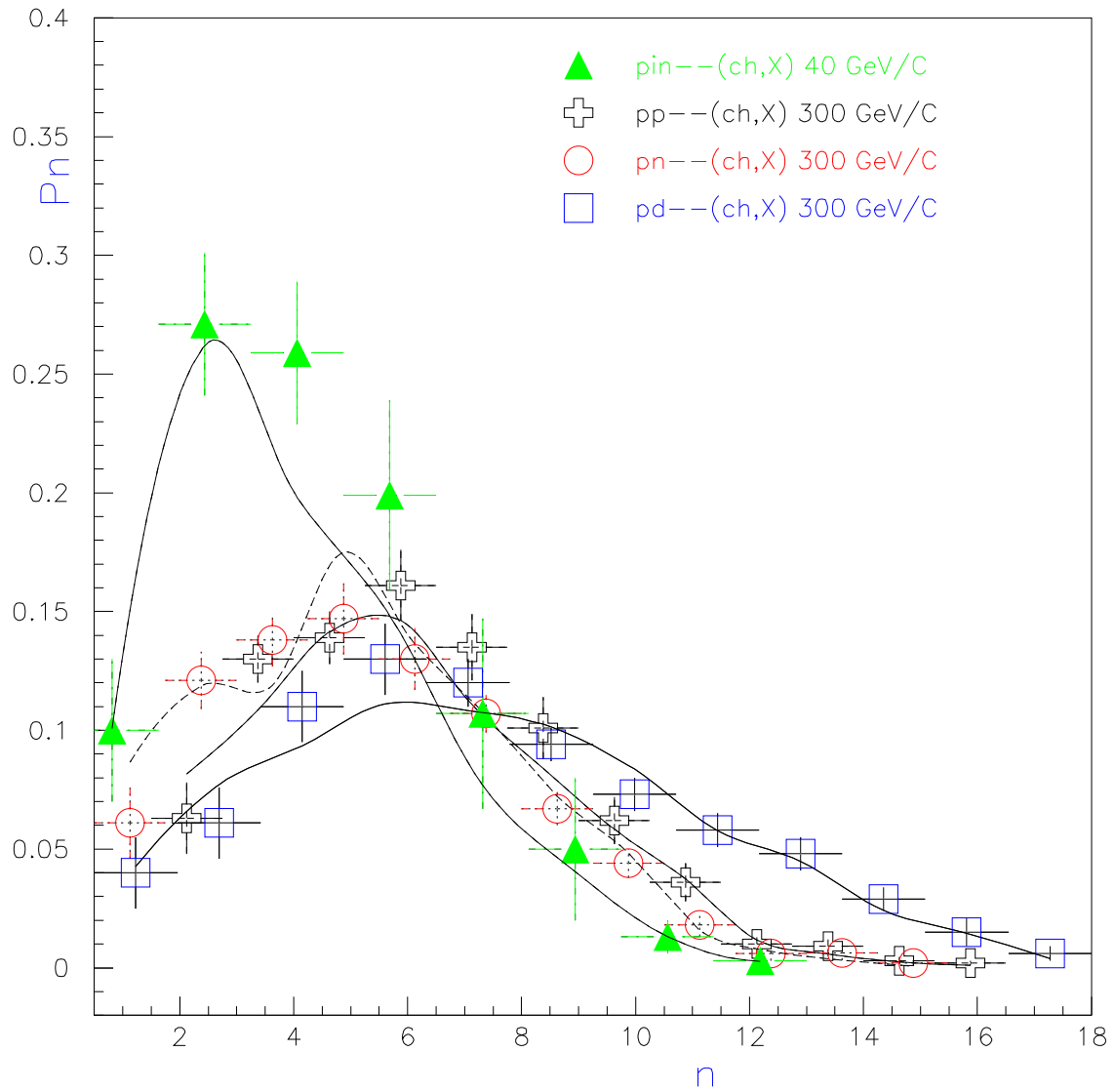


Figure 7: The multiplicity distributions of charged particles (π^- , n) \rightarrow (ch, X) at the momentum of 40 GeV/c/nucleon and ($p, (p, n, d)$) \rightarrow (ch, X) at the momentum of 300 GeV/c/nucleon.

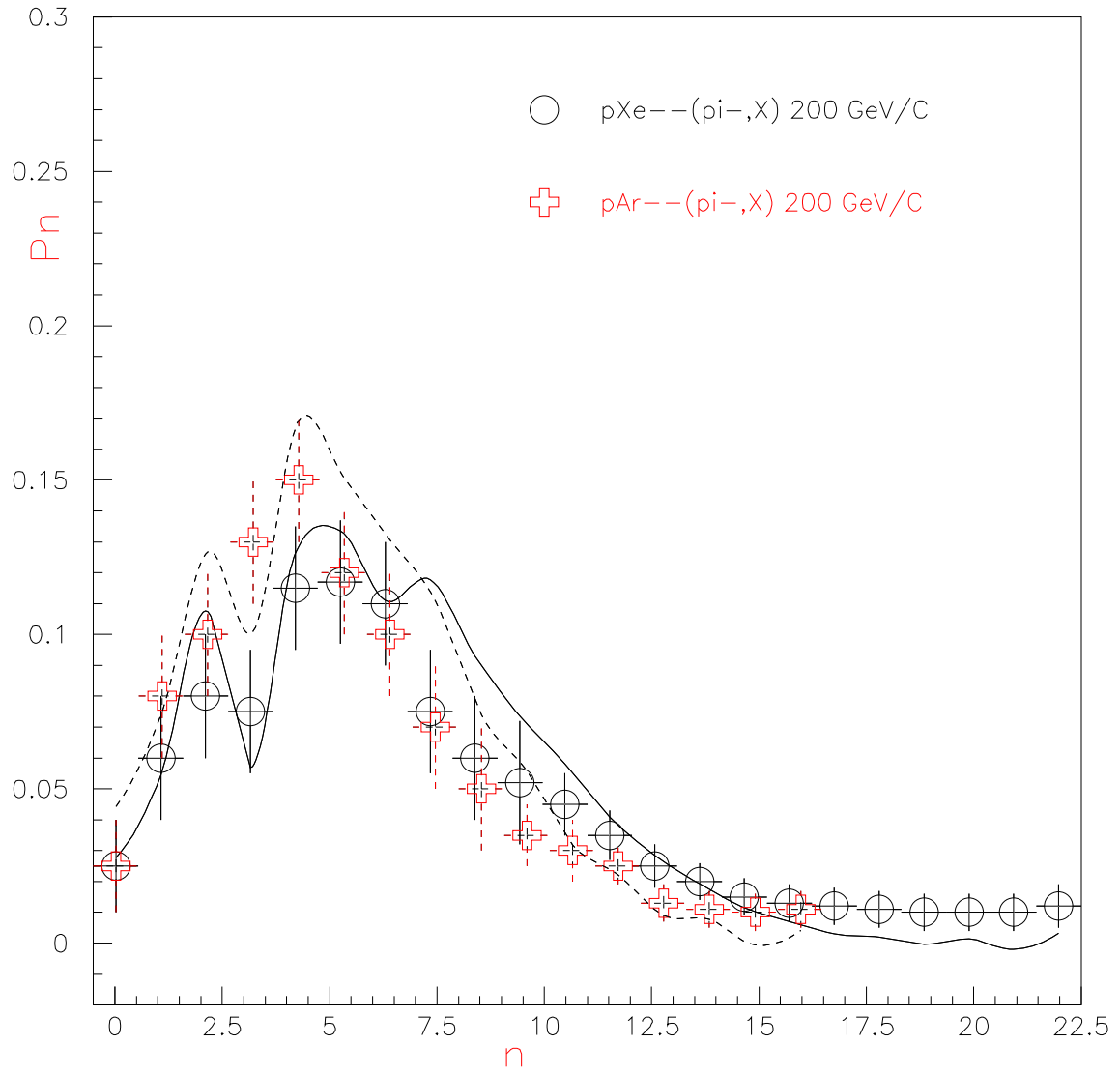


Figure 8: The multiplicity distributions of π^- mesons in $(p, (Ar, Xe)) \rightarrow (\pi^-, X)$ collisions at 200 GeV/c/nucleon.

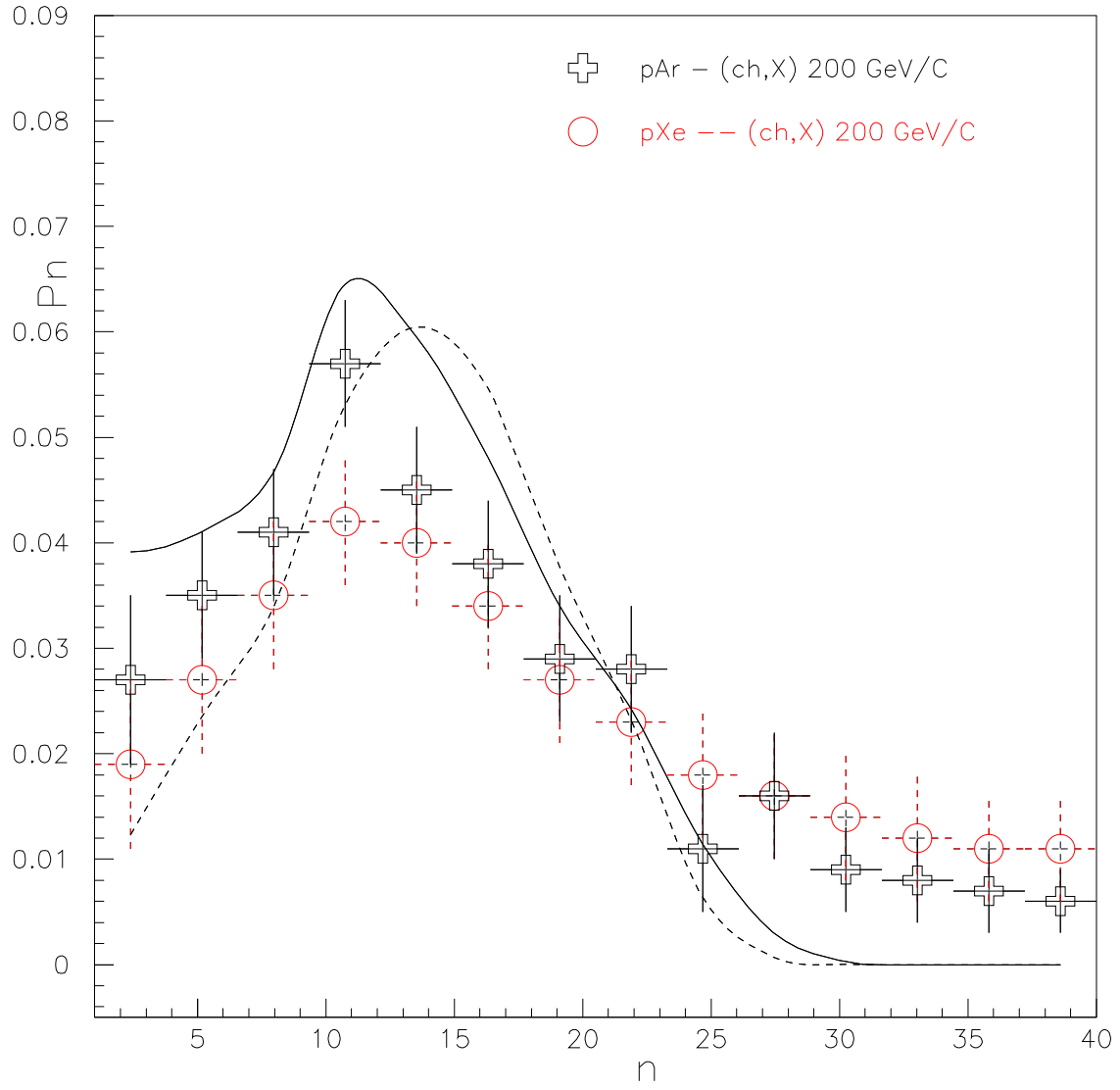


Figure 9: The multiplicity distributions of charged particles in $(p, (Ar, Xe)) \rightarrow (ch, X)$ collisions at 200 GeV/c/nucleon.